

A Cog-Wheel Model for Nuclear-Spin Propagation in Solids

R. BRÜSCHWEILER AND R. R. ERNST

Laboratorium für Physikalische Chemie, ETH Zentrum, 8092 Zürich, Switzerland

Received August 29, 1996

An efficient quantum-mechanical approach is presented for the computation of the short-term propagation of nuclear polarization in many-spin systems, known as spin diffusion, which carries structural information. It is based on the fact that for short time intervals the spin evolution under dipolar coupling can be expressed analytically by rotations in three- and four-dimensional subspaces of the Liouville space. Due to its high computational efficiency, the approach allows the treatment of several dozens of coupled spins and is well suited to the rapid calculation of spin propagation in oriented samples and in powders. © 1997 Academic Press

INTRODUCTION

Monitoring the propagation of nuclear-spin polarization in solids, sometimes termed spin diffusion (1), provides structural information on crystalline and amorphous solids. In spin-propagation experiments the exchange of Zeeman spin order is caused by dipolar spin couplings reflecting internuclear distances and angles. In the past, such information has been successfully extracted using a variety of experimental schemes (2–7).

Spin-diffusion experiments resemble in concept and purpose liquid-state NMR cross-relaxation experiments (8, 9). An important asset of cross relaxation is the capability to back-calculate the cross-relaxation spectrum from a molecular model (10) to readily check for consistency between model and experiment. Structurally most significant is thereby the short-term behavior of cross relaxation in the initial-rate regime (9). For longitudinal spin relaxation of macromolecules in the liquid state, only one-spin order is considered and the cross-relaxation process is described by a master equation for the polarization, which yields for N spins- $\frac{1}{2}$ a set of N coupled linear differential equations. Since the dimension of the problem increases linearly with the number of spins, numerical calculations including several hundred spins are possible and are routinely used for structure refinements of biomolecules [for an overview see (11)].

In the solid state, on the other hand, multispin effects play a crucial role and impede the exact theoretical treatment of spin propagation in large spin systems. A fully quantum-

mechanical treatment is necessary for an accurate description of spin-propagation processes, since it has been demonstrated also experimentally that for short evolution times ^1H spin diffusion is indeed a deterministic, reversible process (12). An exact quantum-mechanical treatment of N dipolar-coupled spins- $\frac{1}{2}$ involves propagator matrices in the zero-quantum space of the dimension $\begin{bmatrix} 2N \\ N \end{bmatrix}$ (9), which renders calculations even for small systems with $N > 10$ prohibitively expensive.

It has been realized from the very beginning that important aspects of spin propagation can also be described with simplified models. Bloembergen (1) formulated the spatial migration of Zeeman order in terms of a diffusion equation. Using perturbation theory, a transition probability for spin flip-flop processes can be derived, involving the zero-quantum lineshape function for the spin pair under consideration (13). Unfortunately, there is at present no satisfactory theory available to calculate this zero-quantum lineshape function for quantitative comparison with experimental data. While a diffusion description is plausible for longer mixing times, it is inappropriate for shorter times due to the unitary character of the underlying process (12). In recent years, computational procedures have been developed on a classical and on a quantum-mechanical basis for the description of spin diffusion (14).

We present here a simplified approach for the accurate calculation of short-term spin propagation. It is well known that for a system of two coupled spins- $\frac{1}{2}$, an analytical solution of the Liouville–von Neumann equation exists: A dipolar interaction H_{12} between spins I_1 and I_2 induces a rotation in a subspace spanned by the one-spin operators I_{1z} , I_{2z} , and the zero-quantum operator $I_{1y}I_{2x} - I_{1x}I_{2y}$. The rotation frequency is determined by the dipolar coupling strength. Extension to a three-spin or larger spin system is *not* straightforward, since H_{12} does not commute with the dipolar interactions H_{13} and H_{23} to a third spin. However, for short times Δt , the propagator $U = \exp[-i\Delta t(H_{12} + H_{13} + H_{23})]$ can be approximated by $\exp(-i\Delta t H_{12})\exp(-i\Delta t H_{13}) \times \exp(-i\Delta t H_{23})$. The geometric analogue is the commutation of infinitesimal rotations about different axes in real space. Hence, for short Δt , U describes independent rota-

tions in the corresponding three-dimensional Liouville subspaces. During Δt the zero-quantum terms $I_{iy}I_{jx} - I_{ix}I_{jy}$ evolve also to zero-quantum terms of the type $I_{iy}I_{kx} - I_{ix}I_{ky}$, $I_{jy}I_{kx} - I_{jx}I_{ky}$, as well as to three-spin terms. These rotations can also be described analytically. In this way, the time evolution of Zeeman order I_{iz} experiences a sequence of rotations in three- and four-dimensional subspaces during successive time intervals Δt . The crucial time-saving feature of the proposed method is the restriction to low-order product-operator terms. Transformations that would lead to higher-order terms are neglected. The evolution consists thus of a series of low-dimensional rotations resembling the mechanism of a system of cog wheels, and we call this approach the ‘‘cog-wheel method.’’

In this work, only three-spin and lower-order terms are considered in the density operator. Extension to higher-order terms is possible at the expense of rapidly increasing computer memory and computational time requirements. Restriction to spin orders that are smaller than the total number of spins implies that the spin-propagation behavior is predictable only for finite evolution times. However, it is the short-term regime which is structurally most informative since multiple-pathway contributions, which tend to intermix the structural information, play a negligible role.

The outline of the remainder of this paper is as follows: In the next section, the general theory is developed. In the following section, the theory is applied to selected geometric arrangements of the nuclear spins and compared with exact quantum-mechanical calculations.

THEORY

We consider a homonuclear system consisting of N spins of $I = \frac{1}{2}$ which are coupled by the secular dipolar interaction between pairs of spins I_i and I_j

$$H_{ij} = \omega_{ij}(2I_{iz}I_{jz} - I_{ix}I_{jx} - I_{iy}I_{jy}) \quad [1]$$

$$\begin{bmatrix} a \\ b \\ c \end{bmatrix} \xrightarrow{H_{ij}\Delta t} \begin{bmatrix} a' \\ b' \\ c' \end{bmatrix} = \begin{bmatrix} (1 + \cos \omega_{ij}\Delta t)/2 & (1 - \cos \omega_{ij}\Delta t)/2 & -(\sin \omega_{ij}\Delta t)/2 \\ (1 - \cos \omega_{ij}\Delta t)/2 & (1 + \cos \omega_{ij}\Delta t)/2 & (\sin \omega_{ij}\Delta t)/2 \\ \sin \omega_{ij}\Delta t & -\sin \omega_{ij}\Delta t & \cos \omega_{ij}\Delta t \end{bmatrix} \begin{bmatrix} a \\ b \\ c \end{bmatrix}. \quad [7]$$

with the dipolar coupling frequency

$$\omega_{ij} = -\frac{\mu_0}{4\pi} \gamma^2 \frac{h}{2\pi} \frac{P_2(\cos \theta_{ij})}{r_{ij}^3} \quad [2]$$

determined by the gyromagnetic ratio γ , the internuclear distance r_{ij} , and the angle θ_{ij} of the internuclear vector with respect to the static magnetic field B_0 . $P_2(x) = (3x^2 - 1)/2$ is the second-rank Legendre polynomial. We neglect the

usually small chemical-shift differences and obtain, in a frame rotating with the Larmor frequency, the Hamiltonian

$$H = \sum_{i < j} H_{ij}. \quad [3]$$

The time evolution of the density operator $\sigma(t)$ will be computed stepwise for small increments Δt , such that the propagator

$$U(\Delta t) = e^{-iH\Delta t} \quad [4]$$

can be approximated, based on the Zassenhaus formula (15), by

$$U \cong \prod_{i < j} \exp(-iH_{ij}\Delta t) \quad [5]$$

despite the noncommutativity of the various terms, $[H_{ij}, H_{ik}] \neq 0$.

In the following, we develop the necessary transformation equations for the individual propagator terms $\exp(-iH_{ij}\Delta t)$. The initial state of the spin system shall be characterized by polarization of spin I_i , $\sigma(0) = I_{iz}$. The evolution under a term H_{ij} follows the transformation

$$I_{iz} \xrightarrow{H_{ij}\Delta t} I_{iz}(1 + \cos \omega_{ij}\Delta t)/2 + I_{jz}(1 - \cos \omega_{ij}\Delta t)/2 + (I_{iy}I_{jx} - I_{ix}I_{jy})\sin \omega_{ij}\Delta t, \quad [6]$$

which represents a well-known rotation in the three-dimensional zero-quantum frame with constant sum polarization $\langle I_{iz} + I_{jz} \rangle$. For an arbitrary initial condition $\sigma_0 = aI_{iz} + bI_{jz} + c(I_{iy}I_{jx} - I_{ix}I_{jy})$, evolving in the time interval Δt to $\sigma(\Delta t) = a'I_{iz} + b'I_{jz} + c'(I_{iy}I_{jx} - I_{ix}I_{jy})$, we find, in matrix notation,

Subsequent propagation of the resulting two-spin terms $I_{iy}I_{jx} - I_{ix}I_{jy}$ under additional dipolar interactions H_{ik} and H_{jk} proceeds also in the form of rotations in low-dimensional subspaces:

$$I_{iy}I_{jx} - I_{ix}I_{jy} \xrightarrow{H_{ik}\Delta t} (I_{iy}I_{jx} - I_{ix}I_{jy})\cos \omega_{ik}\Delta t \cos(\omega_{ik}\Delta t/2)$$

$$\begin{aligned}
& + (I_{jy}I_{kx} - I_{jx}I_{ky}) \sin \omega_{ik}\Delta t \sin(\omega_{ik}\Delta t/2) \\
& - 2(I_{jx}I_{kx} + I_{jy}I_{ky})I_{iz} \cos \omega_{ik}\Delta t \sin(\omega_{ik}\Delta t/2) \\
& - 2(I_{ix}I_{jx} + I_{iy}I_{jy})I_{kz} \sin \omega_{ik}\Delta t \cos(\omega_{ik}\Delta t/2)
\end{aligned} \quad [8]$$

and

$$\begin{aligned}
I_{iy}I_{jx} - I_{ix}I_{jy} & \xrightarrow{H_{jk}\Delta t} \\
& (I_{iy}I_{jx} - I_{ix}I_{jy}) \cos \omega_{jk}\Delta t \cos(\omega_{jk}\Delta t/2) \\
& - (I_{iy}I_{kx} - I_{ix}I_{ky}) \sin \omega_{jk}\Delta t \sin(\omega_{jk}\Delta t/2) \\
& + 2(I_{ix}I_{kx} + I_{iy}I_{ky})I_{jz} \cos \omega_{jk}\Delta t \sin(\omega_{jk}\Delta t/2) \\
& + 2(I_{ix}I_{jx} + I_{iy}I_{jy})I_{kz} \sin \omega_{jk}\Delta t \cos(\omega_{jk}\Delta t/2).
\end{aligned} \quad [9]$$

These transformations produce three-spin terms $2(I_{ix}I_{jx} + I_{iy}I_{jy})I_{kz}$, $2(I_{ix}I_{kx} + I_{iy}I_{ky})I_{jz}$, and $2(I_{jx}I_{kx} + I_{jy}I_{ky})I_{iz}$, which again evolve further into two-spin, three-spin, and four-spin terms under additional dipolar interactions. Here, a key feature of the cog-wheel approach becomes active: We disregard all those further transformations that could produce four-spin terms. This implies that, e.g., the term $2(I_{ix}I_{jx} + I_{iy}I_{jy})I_{kz}$ evolves exclusively under the dipolar Hamiltonians H_{ik} and H_{jk} . All other dipolar terms, such as H_{il} , H_{jl} , and H_{kl} , are disregarded in their effect at this particular stage of evolution. It is easily seen that the Hamiltonian H_{ij} commutes with the above density-operator term and causes no transformation. The two active terms cause the transformations

$$\begin{aligned}
2(I_{ix}I_{jx} + I_{iy}I_{jy})I_{kz} & \xrightarrow{H_{ik}\Delta t} \\
& 2(I_{ix}I_{jx} + I_{iy}I_{jy})I_{kz} \cos \omega_{ik}\Delta t \cos(\omega_{ik}\Delta t/2) \\
& - 2(I_{jx}I_{kx} + I_{jy}I_{ky})I_{iz} \sin \omega_{ik}\Delta t \sin(\omega_{ik}\Delta t/2) \\
& - (I_{jy}I_{kx} - I_{jx}I_{ky}) \cos \omega_{ik}\Delta t \sin(\omega_{ik}\Delta t/2) \\
& + (I_{iy}I_{jx} - I_{ix}I_{jy}) \sin \omega_{ik}\Delta t \cos(\omega_{ik}\Delta t/2)
\end{aligned} \quad [10]$$

and

$$\begin{aligned}
2(I_{ix}I_{jx} + I_{iy}I_{jy})I_{kz} & \xrightarrow{H_{jk}\Delta t} \\
& 2(I_{ix}I_{jx} + I_{iy}I_{jy})I_{kz} \cos \omega_{jk}\Delta t \cos(\omega_{jk}\Delta t/2) \\
& - 2(I_{ix}I_{kx} + I_{iy}I_{ky})I_{jz} \sin \omega_{jk}\Delta t \sin(\omega_{jk}\Delta t/2) \\
& - (I_{iy}I_{kx} - I_{ix}I_{ky}) \cos \omega_{jk}\Delta t \sin(\omega_{jk}\Delta t/2) \\
& - (I_{iy}I_{jx} - I_{ix}I_{jy}) \sin \omega_{jk}\Delta t \cos(\omega_{jk}\Delta t/2).
\end{aligned} \quad [11]$$

The successive and systematic application of these types of rotations leads to the cog-wheel propagation schematically shown in Fig. 1. The solid lines in the figure take into account all conceivable dipolar transformations, while for the broken lines the restriction to the Hamiltonian terms

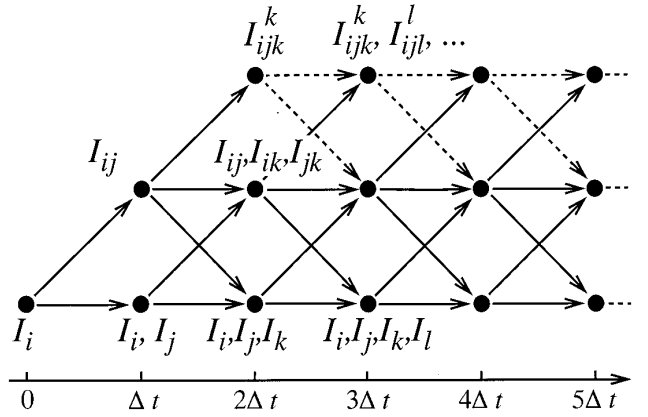


FIG. 1. Schematic view of the cog-wheel approach. Solid arrows indicate evolution under the exact dipolar Hamiltonian H and dashed arrows refer to a subset that restricts the multiple-spin order as discussed in the text. The spin terms are abbreviated according to $I_i \equiv I_{iz}$, $I_{ij} \equiv I_{iy}I_{jx} - I_{ix}I_{jy}$, $I_{ijk}^* \equiv 2(I_{ix}I_{jx} + I_{iy}I_{jy})I_{kz}$.

which do not create four-spin or higher-order terms, as discussed above, applies. The cog-wheel approach allows a highly efficient computation of the short-term evolution. All trigonometric functions can be evaluated at the beginning of the computation and can be stored in a look-up table.

All rotations in the cog-wheel approximation are unitary, leading, on the one hand, to a numerically stable behavior under the iterative application of rotations. This implies, on the other hand, a nonsystematic neglect of higher-order propagator terms: Higher-order powers of individual dipolar terms are taken into account, but products between different dipolar terms are neglected in the propagator of Eq. [5]. This is however of no consequence, provided that the time increment Δt is selected to be sufficiently short (15).

The neglect of four-spin and higher-order terms in the density operator leads to a drastic reduction of the number of basis operators to be considered. While for an unrestricted calculation of spin propagation $Z^{(N)} = \begin{bmatrix} 2N \\ N \end{bmatrix}$ zero-quantum operators are sufficient for an N -spin- $\frac{1}{2}$ system, the restriction to three-spin terms requires only $Z^{(3)} = N + \begin{bmatrix} N \\ 2 \end{bmatrix}$ ($N - 1$) operators. For example, for an eight-spin system, the respective numbers are $Z^{(N)} = 12,870$ and $Z^{(3)} = 204$, which greatly reduces the computational time required. The time-saving is even larger when compared with a straightforward propagation of the full $2^N \times 2^N$ density matrix with 65,536 matrix elements.

On the other hand, the restriction to low spin-order terms prevents calculation of the long-term evolution which necessarily involves higher spin-order terms. For example, in the context of polarization-echo experiments (12), the higher spin-order terms become part of the ‘‘spin memory’’ that

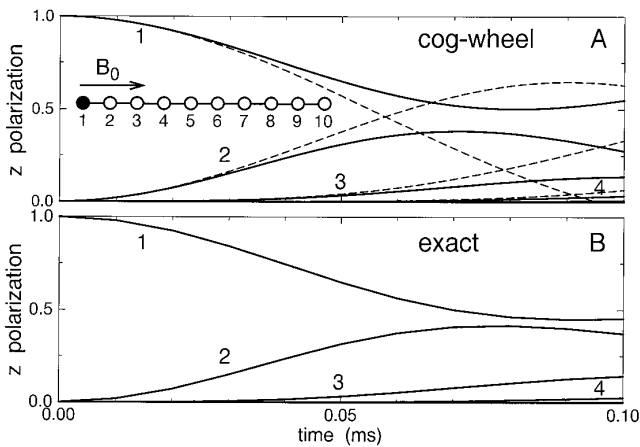


FIG. 2. Comparison of the cog-wheel approach (A) with an exact quantum-mechanical spin calculation (B) for a linear chain of 10 proton spins, which is aligned parallel to the magnetic field B_0 , with spacing between spins of 3 \AA . The time behavior of Zeeman spin order $\langle I_{iz} \rangle$ ($i = 1, \dots, 10$) is shown and the curves are labeled with the corresponding spin number. At $t = 0$, all polarization is concentrated on the first spin: $\sigma(0) = I_{1z}/\text{Tr}\{I_{1z}^2\}$ with $\langle I_{1z} \rangle = 1$. The integration time step Δt was set to $5.0 \times 10^{-7} \text{ s}$. In Panel A the results of a second-order cog-wheel calculation retaining only one-spin and two-spin terms are indicated by dashed lines.

allows the reversal of the time evolution for the creation of an echo. For the simulation of this kind of experiments, exact calculations seem to be indispensable.

NUMERICAL APPLICATIONS

The cog-wheel model is compared here with exact quantum-mechanical calculations. For the exact treatment, the Liouville–von Neumann equation is solved numerically by diagonalization of the total dipolar Hamiltonian $H = \sum_{i<j} H_{ij} = \mathbf{R}^{-1}\mathbf{D}\mathbf{R}$ using the program library GAMMA (16), where \mathbf{D} is a diagonal matrix and \mathbf{R} is a unitary transformation matrix. The time evolution of an initial spin-density operator $\sigma(0)$ is then calculated according to

$$\sigma(t) = \mathbf{R}^{-1} e^{-i\mathbf{D}t} \mathbf{R} \sigma(0) \mathbf{R}^{-1} e^{i\mathbf{D}t} \mathbf{R}. \quad [12]$$

For the calculations given here, all possible pairwise dipolar couplings are accounted for.

First, a linear chain of 10 proton spins is considered which is aligned parallel to the external magnetic B_0 field. The spacing between next neighbors is 3.0 \AA . The evolution of one-spin order for the normalized initial conditions $\sigma(0) = I_{1z}/\text{Tr}\{I_{1z}^2\}$ and $\sigma(0) = I_{5z}/\text{Tr}\{I_{5z}^2\}$ is shown in Figs. 2 and 3, respectively. In the Panels A the approximate cog-wheel results are shown while in Panels B the exact results using Eq. [12] are given. For evolution times shorter than $60 \mu\text{s}$ in Fig. 2 and $40 \mu\text{s}$ in Fig. 3 the difference between the exact and approximate results is smaller than 1.5% of the initial polarization.

In Fig. 3 the initially polarized spin I_5 transfers its polarization more rapidly to its neighbors than spin I_1 in Fig. 2, since I_5 is coupled to two neighbors at a distance of 3 \AA (I_4 and I_6), whereas spin I_1 has only one neighbor spin (I_2). Within the mentioned evolution times the polarization of the initially polarized spin drops to about half of its original value.

It is interesting to compare the third-order cog-wheel approach with the next lower order of approximation, a second-order cog-wheel procedure where only one-spin and two-spin product-operator terms are retained. In Fig. 2A the curves for the second-order approximation are included. It is apparent that the divergence from the exact solution is much more rapid than that for the third-order approximation. For an evolution time of $60 \mu\text{s}$, the deviation from the exact solution is approximately a factor of 10 larger than that for the third-order approximation. In terms of the permitted evolution time for a restricted inaccuracy, the third-order cog-wheel approach allows for an extension by about a factor of 2.

As a second example, six proton spins are placed at the corners of a regular octahedron with side length of 3 \AA . A seventh spin is placed in the center of the octahedron and has a distance of $3/\sqrt{2} \text{ \AA}$ to the other spins. Figure 4 shows the evolution of one-spin z polarization if at $t = 0$ the central spin is polarized $\sigma(0) = I_{1z}/\text{Tr}\{I_{1z}^2\}$. The magnetic B_0 field is applied parallel to a fourfold symmetry axis, leading to a pair and a quartet of equivalent corner spins. The rather high spin density surrounding the central spin causes a fast monotonous drop of its magnetization within about $15 \mu\text{s}$. For this period, the polarization difference between the approximate treatment and the cog-wheel method is smaller than 2% of the initial polarization.

The cog-wheel approach shows a remarkably high computational speed. On an SGI Onyx computer it requires four seconds CPU time for the ten-spin chain while the exact treatment lasts for more than one day.

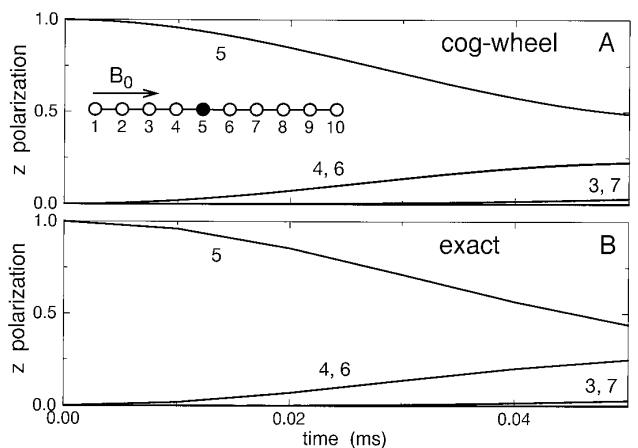


FIG. 3. Same as Fig. 2, but with initial condition $\sigma(0) = I_{5z}/\text{Tr}\{I_{5z}^2\}$ with $\langle I_{5z} \rangle = 1$.

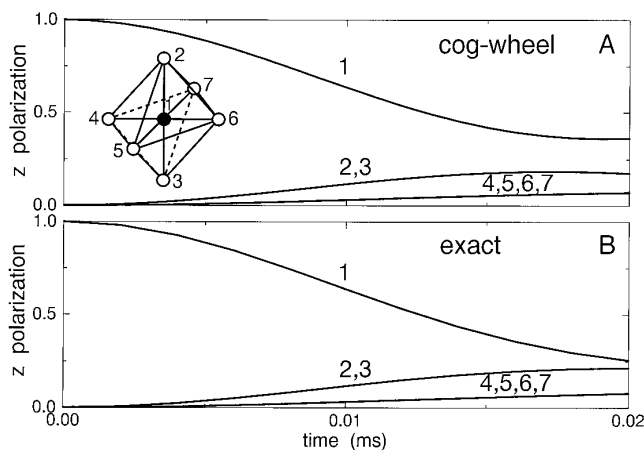


FIG. 4. Comparison of the cog-wheel treatment (A) with an exact quantum-mechanical spin calculation (B) for an octahedron with a side length of 3 Å consisting of seven proton spins (six in the corners and one in the center) depicted in Panel A. The octahedron is oriented such that a fourfold symmetry axis is aligned parallel to the direction of B_0 . At $t = 0$, all polarization is concentrated on the central spin: $\sigma(0) = I_{1z}/\text{Tr}\{I_{1z}^2\}$ with $\langle I_{1z} \rangle = 1$. The integration time step Δt was set to 1.0×10^{-7} s.

CONCLUSION

While the potential of spin propagation as a rich source of structural information has been recognized for decades, the quantitative interpretation of experimental data on larger spin systems was seriously hampered by the computational costs of computer simulations growing exponentially with the size of the spin system. The method presented here allows rapid calculation of the short-term behavior of homonuclear spin propagation for a large number of coupled spins.

The present treatment does not include chemical-shift and chemical-shielding anisotropy effects. While such effects play no significant role in proton systems or in rotating-frame spin-diffusion experiments, they can be incorporated into the cog-wheel method without much difficulty by expanding the set of basis operators. Also, an extension of the method to include four-spin (and possibly even higher-order) terms is conceivable at the costs of a significant increase of computer time and memory.

This work deals with evolution under the dipolar Hamiltonian in the absence of magic-angle sample spinning (MAS). Extraction of dipolar coupling information under MAS conditions requires application of recoupling schemes (17), and the restored effective dipolar Hamiltonian differs from that

of Eq. [1]. While the corresponding transformation rules of Eqs. [7]–[11] need to be modified, the concept of the cog-wheel approach seems still applicable.

The decay of polarization of an initially polarized spin carries information on local molecular structure similar to homonuclear relaxation in liquid-state NMR. Magnetization transfer between protons attached to specifically labeled ^{13}C sites using heteronuclear editing techniques (12), on the other hand, yields specific distance information for both crystalline and amorphous systems. For these types of experiments, the cog-wheel model for spin propagation may help to relate experimental observations more quantitatively to molecular structural models.

ACKNOWLEDGMENTS

We thank Dr. Marco Tomaselli and Sabine Hediger for stimulating discussions. The research has been supported by the Swiss National Science Foundation.

REFERENCES

1. N. Bloembergen, *Physica* **15**, 386 (1949).
2. H. T. Edzes and J. P. C. Bernards, *J. Am. Chem. Soc.* **106**, 1515 (1984).
3. P. M. Henrichs and M. Linder, *J. Magn. Reson.* **58**, 458 (1984).
4. R. Tycko and G. Dabbagh, *J. Am. Chem. Soc.* **115**, 3592 (1991).
5. G. Dabbagh, D. P. Weliky, and R. Tycko, *Macromolecules* **27**, 6183 (1992).
6. P. Robyr, B. H. Meier, and R. R. Ernst, *Chem. Phys. Lett.* **187**, 471 (1991).
7. P. Robyr, B. H. Meier, P. Fischer, and R. R. Ernst, *J. Am. Chem. Soc.* **116**, 5315 (1994).
8. I. Solomon, *Phys. Rev.* **99**, 559 (1955).
9. R. R. Ernst, G. Bodenhausen, and A. Wokaun, "Principles of Nuclear Magnetic Resonance in One and Two Dimensions," Clarendon Press, Oxford, 1987.
10. J. W. Keepers and T. L. James, *J. Magn. Reson.* **57**, 404 (1984).
11. R. Brüschweiler and D. A. Case, *Prog. NMR Spectrosc.* **26**, 27 (1994).
12. S. Zhang, B. H. Meier, and R. R. Ernst, *Phys. Rev. Lett.* **69**, 2149 (1992).
13. A. Abragam, "Principles of Nuclear Magnetism," Clarendon Press, Oxford, 1961.
14. D. K. Sodickson and J. S. Waugh, *Phys. Rev. B* **52**, 6467 (1995).
15. W. Magnus, *Commun. Pure Appl. Math.* **7**, 649 (1954).
16. S. A. Smith, T. O. Levante, B. H. Meier, and R. R. Ernst, *J. Magn. Reson. A* **106**, 75 (1993).
17. A. E. Bennett, R. G. Griffin, and S. Vega, "NMR Basic Principles and Progress," Vol. 33, p. 3, Springer-Verlag, Berlin/Heidelberg, 1994.